Received: 9 May 2020 | Accepted: 1 November 2020

DOI: 10.1111/pce.13939

ORIGINAL ARTICLE

Plant, Cell & Environment

WILEY

Stomatal closure of tomato under drought is driven by an increase in soil–root hydraulic resistance

Mohanned Abdalla[1,2] | Andrea Carminati[1] | Gaochao Cai[1,3] | Mathieu Javaux[4,5] | Mutez Ali Ahmed[1,3]

[1]Chair of Soil Physics, Bayreuth Center of Ecology and Environmental Research (BayCEER), University of Bayreuth, Bayreuth, Germany

[2]Department of Horticulture, Faculty of Agriculture, University of Khartoum, Khartoum North, Sudan

[3]Biogeochemistry of Agroecosystems, University of Göttingen, Göttingen, Germany

[4]Earth and Life Institute-Environmental Science, Universite Catholique de Louvain, Louvain-la-Neuve, Belgium

[5]Agrosphere (IBG-3), Forschungszentrum Juelich GmbH, Juelich, Germany

Correspondence
Mohanned Abdalla and Gaochao Cai, Chair of Soil Physics, Bayreuth Center of Ecology and Environmental Research (BayCEER), University of Bayreuth, Universitätsstraße 30, 95447, Bayreuth, Germany.
Email: mohanned.abdalla-ali-abdalla@uni-bayreuth.de; gaochao.cai@uni-bayreuth.de

Funding information
Deutscher Akademischer Austauschdienst; Bundesministerium für Bildung und Forschung; German Academic Exchange Service (DAAD)

Abstract

The fundamental question as to what triggers stomatal closure during soil drying remains contentious. Thus, we urgently need to improve our understanding of stomatal response to water deficits in soil and atmosphere. Here, we investigated the role of soil–plant hydraulic conductance (K_{sp}) on transpiration (E) and stomatal regulation. We used a root pressure chamber to measure the relation between E, leaf xylem water potential ($\psi_{leaf\text{-}x}$) and soil water potential (ψ_{soil}) in tomato. Additional measurements of $\psi_{leaf\text{-}x}$ were performed with unpressurized plants. A soil–plant hydraulic model was used to simulate $E(\psi_{leaf\text{-}x})$ for decreasing ψ_{soil}. In wet soils, $E(\psi_{leaf\text{-}x})$ had a constant slope, while in dry soils, the slope decreased, with $\psi_{leaf\text{-}x}$ rapidly and nonlinearly decreasing for moderate increases in E. The $\psi_{leaf\text{-}x}$ measured in pressurized and unpressurized plants matched well, which indicates that the shoot hydraulic conductance did not decrease during soil drying and that the decrease in K_{sp} is caused by a decrease in soil–root conductance. The decrease of E matched well the onset of hydraulic nonlinearity. Our findings demonstrate that stomatal closure prevents the drop in $\psi_{leaf\text{-}x}$ caused by a decrease in K_{sp} and elucidate a strong correlation between stomatal regulation and belowground hydraulic limitation.

KEYWORDS
belowground hydraulic, hydraulic conductivity, leaf water potential, soil drying, *Solanum lycopersicum* L., transpiration, water stress

1 | INTRODUCTION

What triggers stomatal closure in plants during soil drying? Water flow across the soil–plant atmosphere continuum is controlled by leaf area, stomatal conductance (g_s [mol m^{-2} s^{-1}]) and atmospheric demand (vapor pressure deficit, VPD [kPa]). Transpiration (E [cm^3/s]) causes a decrease in the leaf xylem water potential ($\psi_{leaf\text{-}x}$ [MPa]) that propagates through the xylem vessels down to the roots and the soil. $\psi_{leaf\text{-}x}$ depends on the soil water potential (ψ_{soil} [MPa]), transpiration rate and the hydraulic conductivities of the elements composing the soil–plant system. It is well accepted that plants continuously adapt to variable atmospheric and soil conditions by altering the hydraulic conductivity of key elements below and above ground, but our understanding of this hydraulic acclimatization is, as yet, incomplete.

Although the underlying mechanisms controlling stomatal regulation at the mechanistic and molecular levels, especially in drying soil, are yet to be fully revealed (Buckley, 2005, 2019), recent studies have demonstrated that we still could anticipate stomatal response to soil drying from its emergent properties (Sperry et al., 2016). Sperry and Love (2015) proposed a 'supply–demand' hydraulic framework to

understand the physical constraints on transpiration. The premise is that stomatal regulation avoids excessive drop in $\psi_{leaf\text{-}x}$ by responding to nonlinearities in the relationship between $\psi_{leaf\text{-}x}$ and E. The nonlinearities and the trigger of stomatal closure have been assumed to be closely coordinated with xylem cavitation (Anderegg et al., 2017; Sperry & Love, 2015). However, other elements of the soil–plant continuum can limit the water transport before xylem cavitates. A recent study on wheat (*Triticum aestivum*) concluded that neither xylem cavitation nor a decrease in leaf conductance drives stomatal closure (Corso et al., 2020). Similarly, Rodriguez-Dominguez and Brodribb (2020) found that the drop of hydraulic conductance of the root–soil interface was the main limitation to water transport and hence represented the primary driver of stomatal closure in olive trees (*Olea europea* L).

Carminati and Javaux (2020) re-proposed the hydraulic model of Sperry and Love (2015) highlighting the role of soil hydraulic conductance (K_s). Using a meta-analysis across species, they showed that the loss of K_s, more than the xylem, coincides better with the stomatal closure. They visualized the relationship between E, $\psi_{leaf\text{-}x}$ and ψ_{soil} as a surface $E(\psi_{leaf\text{-}x},\psi_{soil})$ and hypothesized that stomatal regulation prevents plants to cross the onset of hydraulic nonlinearity. They supported their hypothesis with literature data, which show a linear relationship between E and the difference between $\psi_{leaf\text{-}x}$ and ψ_{soil}. However, existing data failed to prove that stomata close at the onset of hydraulic nonlinearity. In other words, most of the existing evidence indicates that stomata close before the occurrence of hydraulic nonlinearity. Reviews and meta-analysis approaches have addressed this question with emphasis on above-ground components (Bartlett et al., 2016; Martin-StPaul et al., 2017); however, there is still a need for systematic experiments to explore the role of below-ground hydraulic processes in stomatal regulation. The question is: do stomata close at the point when the hydraulic conductance starts to decrease?

Answering this question requires a method to explore the nonlinear part of the $E(\psi_{leaf\text{-}x})$ relation. This is achievable by the root pressure chamber apparatus (Cai et al., 2020; Passioura, 1980). The method provides accurate and high temporal resolution measurements of $\psi_{leaf\text{-}x}$ and E in intact plants with no (or very limited) stomatal regulation. By pressurizing the soil and thus maintaining the leaf turgid, we explored the nonlinear part of the relationship between $\psi_{leaf\text{-}x}$ and E. Furthermore, pressurization prevents cavitation during the increase in E (Passioura & Munns, 1984). Yet, below-ground conductances are not affected by pressurization, including the potential shrinkage of the root cortex and the loss of contact to the soil. Therefore, this method evaluates accurately the changes in below-ground hydraulic conductance occurring at a given E and ψ_{soil} (Carminati et al., 2017; Passioura, 1980). In parallel, we measured the decrease of E and $\psi_{leaf\text{-}x}$ in non-pressurized plants. By comparing $\psi_{leaf\text{-}x}$ in pressurized and unpressurized plants at the same ψ_{soil} and E, we obtain information on the decrease in shoot hydraulic conductance and xylem cavitation (both prevented in pressurized plants). Additionally, by comparing pressurized and non-pressurized experiments, we tested the hypothesis that stomata close at the onset of hydraulic limitation. We applied this method to tomato plants in a sandy-loam soil. The data were interpreted using the conceptual and numerical soil–plant hydraulic model of Carminati and Javaux (2020).

2 | MATERIALS AND METHODS

2.1 | Plant and soil

Tomato (*Solanum lycopersicum* L.) seeds were soaked in H_2O_2 solution for 3 mins and then germinated in petri dishes for 5 days. Plants were grown in polyvinyl chloride (PVC) columns with 30 cm height, 10 cm outer diameter and 9.4 cm inner diameter. Five holes, with a diameter of 5 mm, were made on the column's side for soil moisture measurements. The PVC columns were topped with a 0.8-cm-thick aluminum plate with a centered-hole of 1.4 cm in diameter (Figure S1).

Plants were grown in a climate-controlled room for 3 weeks, with a day/night temperature of 28/18°C, relative humidity of 57/65% and 14 hrs as the photoperiod. The light intensity (LI) was 600 μmol m^{-2} s^{-1} (Luxmeter PCE-174, Meschede, Germany). Plants were watered every 2–3 days to maintain wet soil conditions (θ 0.2 cm^3/cm^3). Preparatory to the experiments, plants were translocated to the laboratory and stems around the collar were glued (UHU plus Endfest 300, Bühl, Germany) to facilitate the forthcoming root pressurization (Figure S1).

The substrate consisted of a mixture of quartz sand and loamy soil with a ratio of 3:5. The substrate was dried at 60°C for 48 hrs and then sieved separately at 1 mm. The water retention and unsaturated hydraulic conductivity curves of the soil mixture are reported in Cai et al. (2020). The soil water content (θ [cm^3/cm^3]) was monitored during the experiment using a time-domain refractometer (TDR) that consists of two rods (length: 6 cm, spacing: 0.5 cm) connected to a data logger (E-Test, Lublin, Poland). Leaves were imaged and analysed using ImageJ (ImageJ 1.50e http://imagej.nih.gov/ij) to estimate leaf area (Skelton et al., 2017). The roots were washed after the experiments and then scanned (with a scanner Epson STD 4800, at a resolution of 400 dpi) to determine the total root length using WinRhizo (Regent Instruments Inc., Canada).

2.2 | Leaf xylem water potential measurements via the root pressure chamber system

We used a root pressure chamber to continuously monitor $\psi_{leaf\text{-}x}$ for varying LI which yielded a varying E (after Passioura, 1980). The detailed construction and calibration were recently introduced in Cai et al. (2020). Briefly, it comprises a root pressure chamber (a metallic cylinder with the dimension of 31.5 cm in height and 17.5 cm in diameter) with a cuvette on top and the main controller unit. The cuvette was equipped with four groups of light-emitting diode (LED) lamps that were attached vertically to the cuvette. LI was measured using a radiometric sensor (Gamma Scientific, San Diego, USA). The airflow passed constantly through the cuvette at a velocity of 8 L/min and was stirred by a small fan. The temperature and the relative humidity

of the inward and outward air were measured with combined temperature–humidity sensors (Galltec-Mela, Bondorf, Germany).

$\psi_{leaf\text{-}x}$ was determined by applying sufficient pneumatic pressure to the root pressure chamber to bring the water in a cut leaf to atmospheric pressure. This applied pressure, called the balancing pressure (P [MPa]), is numerically equal to minus the suction in leaf xylem before pressurization at the same transpiration rate E (Cai et al., 2020; Carminati et al., 2017; Passioura, 1980). A meniscus system that encompasses a capillary tube and an infrared detector was attached to the leaf cut (petiolule) to maintain the hydraulic connection to observe P. $\psi_{leaf\text{-}x}$ was determined when the meniscus was stable for at least 10 mins (Cai et al., 2020). E was calculated by multiplying the airflow by the difference between the outward and inward humidity.

Experiments were started with positioning the columns inside the pressure chamber and the shoots in the cuvette. E was altered by changing LI from 0 μmol m^{-2} s^{-1} to 200, 400, 600, 800 and 1,000 μmol m^{-2} s^{-1}. The corresponding $\psi_{leaf\text{-}x}$ was determined at each E. The full cycle of LI was achieved only in wet soils because in dry soils $\psi_{leaf\text{-}x}$ could not be sustained at high E.

Additionally, we measured $\psi_{leaf\text{-}x}$ and E in unpressurized plants. E was measured using the same cuvette as explained above. $\psi_{leaf\text{-}x}$ was measured using a Scholander bomb (Soil Moisture Equipment corp. Santa Barbara, CA., USA).

2.3 | Soil–plant hydraulic model

We used a simplified model of water flow in the soil–plant continuum. The series of resistances between the bulk soil, soil–root interface and through the root to the leaf xylem were considered in the soil–plant hydraulic model, assuming that one single root represents all active roots that took up water. A detailed description of the model can be found in Carminati and Javaux (2020), Cai et al. (2020), Hayat et al. (2020) and supplementary note S1 and Table S1.

Briefly, the model calculates the gradient in water potential through the soil and along the plant till the leaf. Soil water flow is simulated assuming a radial geometry and an uniform root water uptake into a fraction of the total root length. The water flow in the plant is calculated assuming a proportionality between the plant hydraulic conductance (K_{plant} [cm^3 s^{-1} MPa^{-1}]) and the difference in water potential between the root–soil interface and the leaf, with K_{plant} dropping according to a power law at a given xylem water potential (which is the point at which the xylem starts to cavitate—Equation S5). K_{plant} is given by the harmonic mean of the root conductance K_{root} and the xylem conductance K_x. Solving the flow Equation (S2), we obtain the surface E ($\psi_{leaf\text{-}x}$,ψ_{soil}). The soil–plant conductance K_{sp} is given by the ratio between E and the difference between $\psi_{leaf\text{-}x}$ and ψ_{soil}:

$$K_{sp} = \frac{E}{\psi_{soil} - \psi_{leaf-x}} \quad (1)$$

We defined the onset of hydraulic limitation (SOL) as E at which $\left.\frac{\partial E}{\partial \psi_{leaf-x}}\right|_{\psi_{soil}}$ reaches 70% of its maximum value at a given ψ_{soil} (i.e., at E = 0). Note that the value of 70% is somehow arbitrary. We used it because it indicates a significant change of the conductance. A value between 60 and 80% would give a similar shape for SOL, although slightly shifted.

To match the measured E($\psi_{leaf\text{-}x}$,ψ_{soil}), we inversely modeled the E ($\psi_{leaf\text{-}x}$,ψ_{soil}) relation by varying K_{plant} and the active root length.

3 | RESULTS

In wet soils (θ > 0.114), the relation between leaf xylem water potential ($\psi_{leaf\text{-}x}$) and transpiration (E) had a constant slope (Figure 1). As the soil progressively dried, E($\psi_{leaf\text{-}x}$) became nonlinear, with $\psi_{leaf\text{-}x}$ rapidly and nonlinearly decreasing for small increases in E. The slope of the E ($\psi_{leaf\text{-}x}$) relation was nearly constant in wet soils, with the slope being equal to K_{plant} (6.25×10^{-7} cm^3 s^{-1} MPa^{-1}), and decreased as the soil dried, indicating a decrease in K_{sp}.

The intercept of the E ($\psi_{leaf\text{-}x}$) relation with the axis E = 0, here defined as the predawn leaf xylem water potential ($\psi_{leaf\text{-}x\ PD}$), deviated from the soil matric potential (ψ_{soil}) estimated from the measured θ and the retention curve (Figure 2). Note that $\psi_{leaf\text{-}x\ PD}$ is not simply expected to be equal to the averaged ψ_{soil} but to a ψ_{soil} that is weighted according to root length distribution (Couvreur et al., 2012). Here, we also neglected the gravitational potential, which for our sample size is justified for pressure differences above 0.01 MPa. We come back to the difference between $\psi_{leaf\text{-}x\ PD}$ and ψ_{soil} in the discussion.

E decreased as the soil dried in both pressurized and non-pressurized plants, but in non-pressurized plants, the decrease was much more marked (Figure 3). E slightly decreased also in pressurized plants despite water in the leaf xylem was kept at atmospheric pressure. However, the difference is not significant.

$\psi_{leaf\text{-}x}$ in pressurized and unpressurized plants was similar under the same E and θ, with values close to the 1:1 line (r^2 = .7) (Figure 4). This means that the plant conductance (K_p) did not change under plant pressurization. This implies that there was no significant decrease in

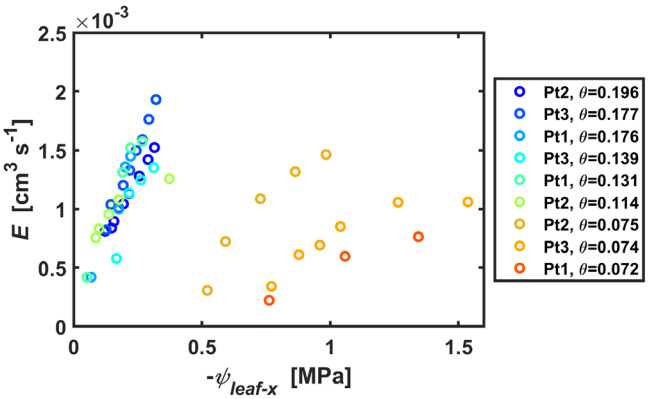

FIGURE 1 Relation between leaf xylem water potential ($\psi_{leaf\text{-}x}$) and transpiration (E) for different soil water contents (θ: cm^3/cm^3). The relation shifts from linear to nonlinear during soil drying. Pt: plant number, n = 3

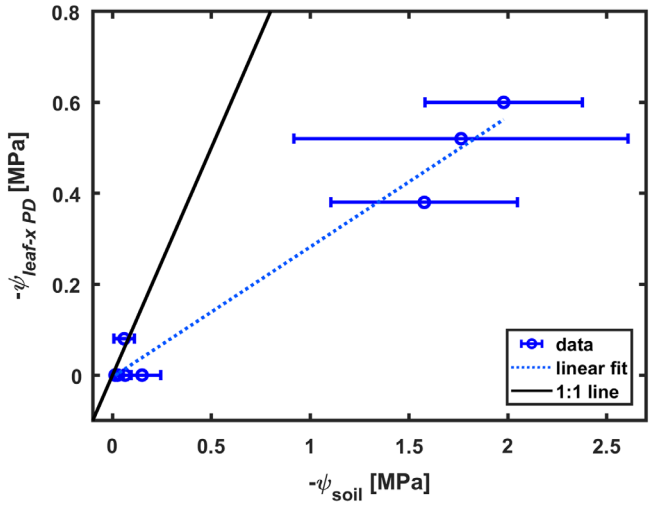

FIGURE 2 Predawn leaf water potential ($\psi_{\text{leaf-x PD}}$), obtained from the intercept of $E(\psi_{\text{leaf-x}})$ with $E = 0$, against the soil matric potential (ψ_{soil}) obtained from the measured soil water contents (θ) and the water retention curve. The dashed line is the best linear fit. The solid line is 1:1 line. In each sample, θ was measured five times and ψ_{soil} was calculated from each of them [Colour figure can be viewed at wileyonlinelibrary.com]

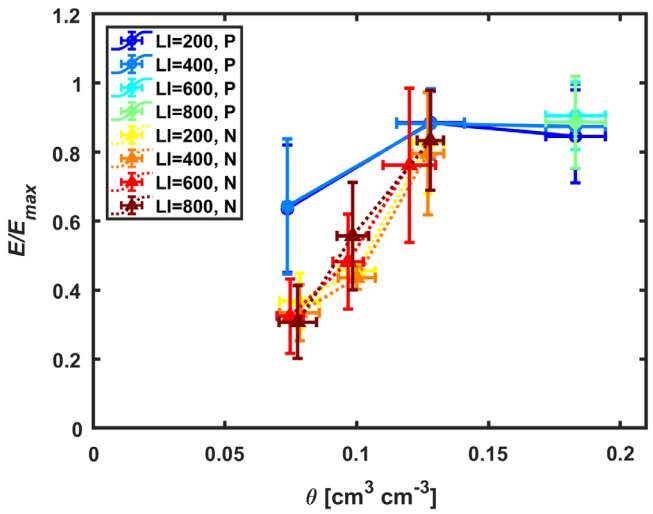

FIGURE 3 Normalized transpiration rate (E/E_{max}) during soil drying (θ: soil water content) under different light intensities (LI: μmol m^{-2} s^{-1}) for pressurized plants (P) and non-pressurized plants (N). Each point is the mean of three plants [Colour figure can be viewed at wileyonlinelibrary.com]

the conductivities of shoot and xylem vessels during soil drying. We will come back to this important point in the discussion.

The soil–plant hydraulic model was able to reproduce the observed $E(\psi_{\text{leaf-x}})$ relation. To match the measurements, the active root length was reduced to 20 m, while the measured one was 75.4 ± 1.3 m ($n = 3$). The water retention curve and soil hydraulic conductivity used in the model are shown in Figure 5. The Brooks–Corey parameterization, used in the soil–plant model (blue line), fits well the measured hydraulic properties (red line) in the range of soil water

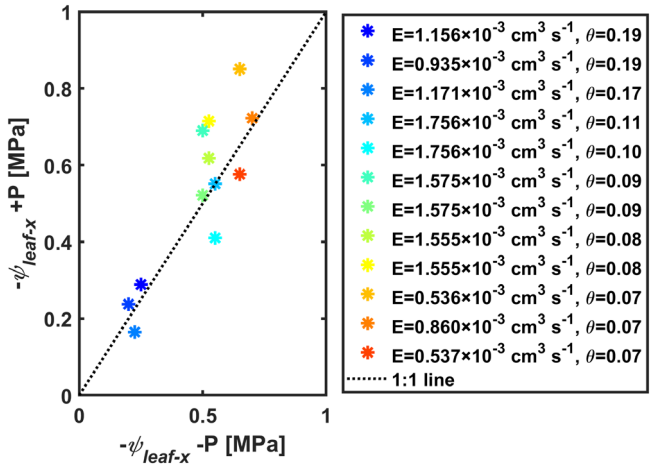

FIGURE 4 Comparison of leaf water potential ($\psi_{\text{leaf-x}}$) in pressurized (+P) and unpressurized (−P) plants at the same soil water content (θ [cm^3/cm^3]) and transpiration (E [cm^2/s]). r^2 = .7. $\psi_{\text{leaf-x}}$ of pressurized plant was measured by the root pressure chamber system, while ψ_{xylem} of unpressurized plants was measured by the Scholander leaf pressure chamber [Colour figure can be viewed at wileyonlinelibrary.com]

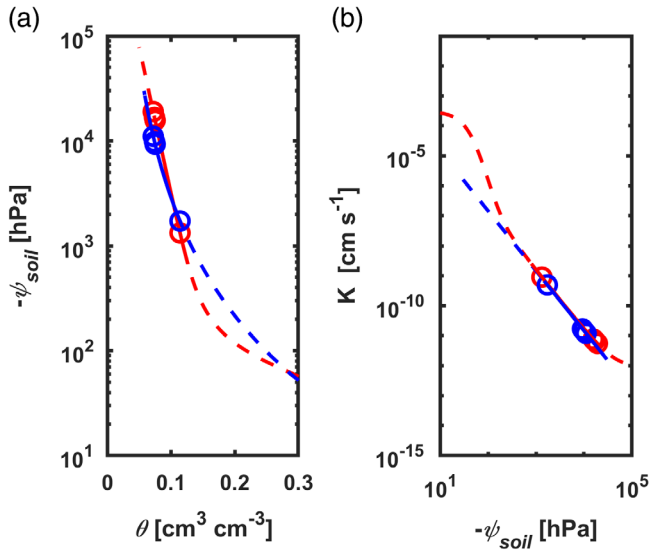

FIGURE 5 (a) Soil water retention curve as fitted with the van Genuchten parameterization (red) and Brooks and Corey model (blue) (Brooks & Corey, 1966; van Genuchten, 1980). The solid part of the lines shows the range of water content (θ) relevant for the experiment. (b) Unsaturated hydraulic conductivities (K) fitted with the Peters-Durner-Iden parameterization (red) and with a power-law relation (Equation S5, blue) (Peters, Iden, & Durner, 2015) [Colour figure can be viewed at wileyonlinelibrary.com]

contents and soil water potential relevant for the experiments (blue solid line) (Brooks & Corey, 1966).

The same set of parameters was used to fit the three plants at all water contents. The onset of hydraulic limitation was defined when $\left.\frac{\partial E}{\partial \psi_{\text{leaf-x}}}\right|_{\psi_{\text{soil}}}$ reached 70% of its maximum value and it is plotted as a red line in Figure 6a,b.

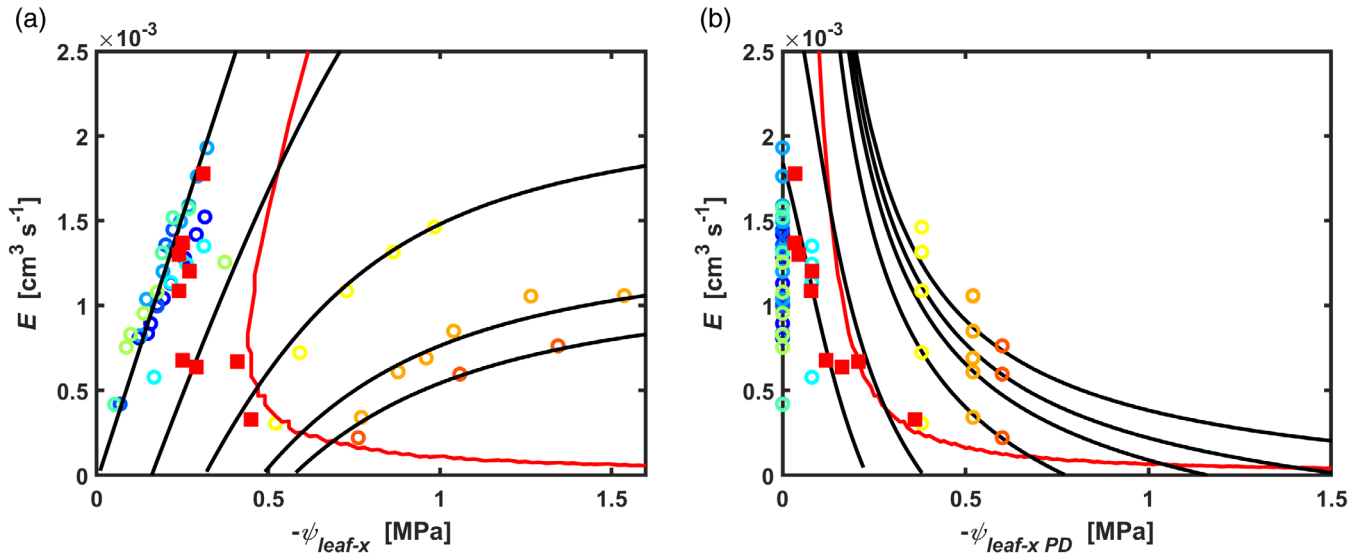

FIGURE 6 Measured (open circles) and fitted (black lines) relationship between transpiration rate (E), leaf xylem water potential ($\psi_{leaf\text{-}x}$) and soil water potential (here replaced by the pre-dawn leaf water potential; $\psi_{leaf\text{-}x\ PD}$). The relation is plotted as (a) the plant view $E(\psi_{leaf\text{-}x})$ and as (b) the soil view $E(\psi_{leaf\text{-}x\ PD})$. The point at which the slope of $E(\psi_{leaf\text{-}x})$ reaches 70% of its maximum value is marked by the red line (onset of hydraulic limitation) in both (a) and (b). The transpiration rates and leaf water potentials of unpressurized plants during soil drying are shown as red squares (three plants at three soil water contents) [Colour figure can be viewed at wileyonlinelibrary.com]

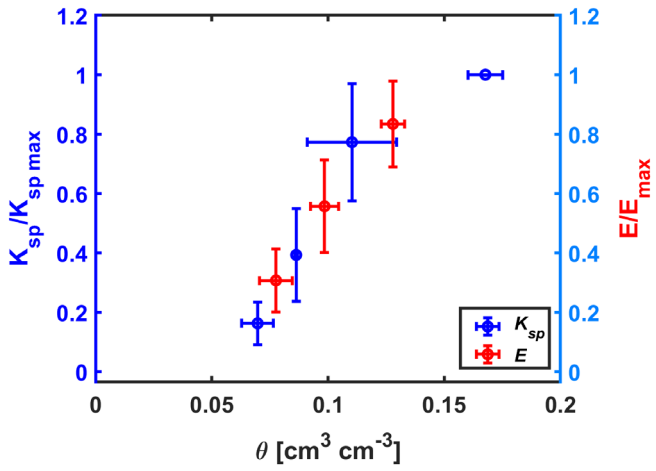

FIGURE 7 The drop in soil–plant hydraulic conductance (K_{sp}) matches the reduction in transpiration (E) during soil drying (θ: soil water content, cm^3/cm^3). K_{sp} was determined at the maximum measured E of the pressurized plants. E was obtained at the light intensity of 800 μmol m^{-2} s^{-1} without pressurization [Colour figure can be viewed at wileyonlinelibrary.com]

The model allows to reconstruct the surface $E(\psi_{leaf\text{-}x},\psi_{soil})$ and to plot E as a function of ψ_{soil} (Figure 6b). In Figure 6b, we used $\psi_{leaf\text{-}x\ PD}$ instead of ψ_{soil} estimated from the TDR and the water retention curve. The reasons are discussed later in the discussion section. In Figure 6, we included E and $\psi_{leaf\text{-}x}$ measured in unpressurized plants at the maximum LI of 800 μmol m^{-2} s^{-1} (red squares obtained from three plants at three water contents—same data as those shown in Figure 3). The decrease in E for decreasing leaf and soil water potentials matches well with the onset of hydraulic limitation (red line), showing a strong correlation (r^2 = .6) between stomatal closure and hydraulic limitation. Note that we do not claim that stomatal closure is always at the onset of hydraulic limitations, but rather that stomatal conductance does not cross the hydraulic limitation represented by the SOL line.

Figure 7 shows an additional way to compare the decrease of E to the soil–plant hydraulic limitation. K_{sp} was normalized by the highest K_{sp} (K_{sp_max}) at the highest θ. E was normalized by the highest E at the same light intensity. E was measured in unpressurized plants, while K_{sp} was obtained from pressurized plants. The results are plotted for different soil water contents. The decline in normalized K_{sp} matched very well the reduction in normalized E (r^2 = .9). This shows that stomatal closure corresponds to a decrease in K_{sp}.

4 | DISCUSSION

In tomato, $E(\psi_{leaf\text{-}x})$ was linear in wet soils, which is in line with the studies on wheat (Deery et al., 2013; Passioura, 1980), barley (Carminati et al., 2017), maize (Hayat et al., 2020), pearl millet (Cai et al., 2020) and lupin (Hayat et al., 2019). The linearity is explained by the fact that in wet soils, the plant hydraulic conductance is constant and lower than that of the soil, thereby controlling the water flow. As the soil dried, its conductivity decreased by several orders of magnitude and the $E(\psi_{leaf\text{-}x})$ relation became nonlinear which is in line with previous studies on wheat, barley and maize (Carminati et al., 2017; Hayat et al., 2020; Passioura, 1980).

The nonlinearity of $E(\psi_{leaf\text{-}x})$ and the associated decline in K_{sp} were concomitant with stomatal closure. This is shown by the good

match between the onset of hydraulic limitation and independent measurements of transpiration response to soil drying (Figure 6), as well as by parallel responses of E and K_{sp} to decreasing soil water content. These results support the hypothesis by Sperry and Love (2015) and Carminati and Javaux (2020) that stomatal closure is triggered by a drop in K_{sp}.

K_{sp} decreased at relatively high leaf xylem water potential (the maximum value of the red line is −0.39 MPa in Figure 6) compared to the value of −1.0 MPa that was recently reported to cause an embolism in tomato (Skelton et al., 2017). In our model, the water potential at which the xylem cavitates was set to −1.5 MPa (ψ_{0x} in Equation S9), which is in the most negative range of leaf xylem water potentials that we simulated, which means that we could have chosen a more negative value without affecting the results. As the water in the leaf xylem was maintained at atmospheric pressure during the measurements of $E(\psi_{leaf\text{-}x})$, the risk of cavitation was reduced (Passioura & Munns, 1984). Moreover, K_{sp} was not substantially affected by pressurization, which is shown by the high correlation (r^2 = .7) between the measurements of leaf xylem water potential of pressurized and unpressurized plants (Figure 4). The fact that K_{sp} was identical in pressurized and unpressurized plants suggests that its decline in drying soils took place belowground, as neither the xylem nor the shoot was affected by a decline in water pressure.

The decline in K_{sp} at a relatively high $\psi_{leaf\text{-}x}$ indicates a marked vulnerability to soil drying (Figure 6). The root length density was relatively small (2.5 cm/cm^3) compared to the value of 13.5 cm/cm^3 measured in pearl millet (Cai et al., 2020). This might explain the drop in K_{sp} at a relatively high $\psi_{leaf\text{-}x}$. This result could be reproduced by the model imposing a root length of 20 m, which corresponds to ca. 25% of the measured root length (75.4 m ± 1.3). The simulations support the hypothesis that the hydraulic decline was caused by water potential dissipation in the soil (Equation S7). An additional cause of the hydraulic decline is root shrinkage and the formation of air-filled gaps at the root–soil interface (Carminati et al., 2013; Rodriguez-Dominguez & Brodribb, 2020). Plants developed strategies, for example, root hairs and mucilage exudation, to bridge gaps and hence soften the drop of the matric potential at the root–soil interface (Ahmed et al., 2018; Carminati et al., 2016). However, tomato has been reported to have short root hairs (ca. 120 μm; Guo et al., 2009), which might hinder their ability to bridge the hydraulic break between soil and roots and prevent the drop in the matric potential across the rhizosphere. Our data do not allow to conclude on what is the main limitation on water flow to the root. So, it is not clear whether the main limitation to water uptake is in the soil or across the root–soil interface. Additional research is needed to investigate the effects of root shrinkage on water fluxes.

Pressurization increased E at low soil water content (θ < 0.12), as it maintained leaf turgidity. This finding is in line with previous studies in wheat, sunflower (Gollan et al., 1986), maize (Hayat et al., 2020) and pearl millet (Cai et al., 2020). Still, a trend in stomatal closure under severe drying (see the reduced E at θ < 0.07; Figures 1, 3 & 6) is visible even in pressurized plants, as previously shown in Gollan et al. (1986), Holbrook et al. (2002) and Cai et al. (2020). At such negative soil water potentials, a root signal might be responsible for the moderate stomatal closure despite the leaves being turgid (Dodd, 2005). However, it might also be that during the measurements, the increase in suction could not be instantaneously balanced by the applied pressure inducing a temporary loss of turgidity in the leaves. Additionally, as plants were not pressurized throughout the whole period of soil drying (which took some days), it might be that ABA produced before plant pressurization was still present in the plant tissues.

In terms of soil water potential, transpiration decreased to ca. its 50% value at $\psi_{leaf\text{-}x\ PD}$ of −0.2 MPa, which was less negative than the expected ψ_{soil} (Figure 2). The deviations could be caused by a more negative osmotic potential in the xylem than in the soil (Cai et al., 2020; Carminati et al., 2017) which would cause the suction in the xylem to be lower than that expected based on the soil matric potential. Note that we measured only the pressure component of the $\psi_{leaf\text{-}x}$ (neglecting the osmotic ones). Another reason is the inaccuracy of estimating ψ_{soil} based on measurements of soil water content and water retention curve. Firstly, the water retention curve was measured in unplanted pots, and root growth might have impacted the water retention curve. Second, averaging the soil water content through the column and assigning it to a water potential is not an obvious operation, and it is likely to differ from the average soil water potential felt by the plant. The fact that $\psi_{leaf\text{-}x\ PD}$ was less negative that ψ_{soil} might indicate that roots were radially more conductive in the wettest soil layers. Accurate measurements of water content (or/and water potential) distribution in the root zone will be needed to better resolve the question on the deviation of $\psi_{leaf\text{-}x\ PD}$ from ψ_{soil}.

In summary, we have shown that, as the soil dried, the relation between leaf xylem water potential and transpiration rate became markedly nonlinear, indicating a drop in K_{sp}. The loss of K_{sp} was primarily explained by a decrease in the soil–root conductance. The decrease in soil–root conductance was concomitant with the reduction in transpiration. This confirms the hypothesis that stomata respond to a decrease in soil–plant hydraulic conductance during soil drying. This stomatal regulation is needed to allow plants to cope with the inherent nonlinearity of the soil–plant hydraulics.

ACKNOWLEDGMENT

The doctoral position of Mohanned Abdalla was funded by the German Academic Exchange Service (DAAD). The position of Gaochao Cai was funded by the Bundesministerium für Bildung und Forschung, Project 02WIL1489 (Deutsch-Israelische Wassertechnologie-Kooperation). Open access funding enabled and organized by Projekt DEAL.

CONFLICT OF INTEREST

The authors declare no conflict of interest.

AUTHOR CONTRIBUTION

All authors conceptualized the study. Mohanned Abdalla conducted the experiments and wrote the manuscript with the contribution of Andrea Carminati, Gaochao Cai, Mathieu Javaux, and Mutez Ali Ahmed.

ORCID

Mohanned Abdalla https://orcid.org/0000-0002-4220-8761

REFERENCES

Ahmed, M. A., Passioura, J., & Carminati, A. (2018). Hydraulic processes in roots and the rhizosphere pertinent to increasing yield of water-limited grain crops: A critical review. *Journal of Experimental Botany*, *69*, 3255–3265.

Anderegg, W. R. L., Wolf, A., Arango-Velez, A., Choat, B., Chmura, D. J., Jansen, S., … Pacala, S. (2017). Plant water potential improves prediction of empirical stomatal models. *PLoS One*, *12*, e0185481.

Bartlett, M. K., Klein, T., Jansen, S., Choat, B., & Sack, L. (2016). The correlations and sequence of plant stomatal, hydraulic, and wilting responses to drought. *Proceedings of the National Academy of Sciences*, *113*, 13098–13103.

Brooks, R. H., & Corey, A. T. (1966). Properties of porous media affecting fluid flow. *Journal of the Irrigation and Drainage Division*, *92*, 61–90.

Buckley, T. N. (2005). The control of stomata by water balance. *New Phytologist*, *168*, 275–292.

Buckley, T. N. (2019). How do stomata respond to water status? *New Phytologist*, *224*, 21–36.

Cai, G., Ahmed, M. A., Dippold, M. A., Zarebanadkouki, M., & Carminati, A. (2020). Linear relation between leaf xylem water potential and transpiration in pearl millet during soil drying. *Plant and Soil*, *447*, 565–578.

Cai, G., Ahmed, M. A., Reth, S., Reiche, M., Kolb, A., & Carminati, A. (2020). Measurement of leaf xylem water potential and transpiration during soil drying using a root pressure chamber system. *Acta Horticulturae*.

Carminati, A., & Javaux, M. (2020). Soil rather than xylem vulnerability controls Stomatal response to drought. *Trends in Plant Science*, *25*, 868–880.

Carminati, A., Passioura, J. B., Zarebanadkouki, M., Ahmed, M. A., Ryan, P. R., Watt, M., & Delhaize, E. (2017). Root hairs enable high transpiration rates in drying soils. *New Phytologist*, *216*, 771–781.

Carminati, A., Vetterlein, D., Koebernick, N., Blaser, S., Weller, U., & Vogel, H.-J. (2013). Do roots mind the gap? *Plant and Soil*, *367*, 651–661.

Carminati, A., Zarebanadkouki, M., Kroener, E., Ahmed, M. A., & Holz, M. (2016). Biophysical rhizosphere processes affecting root water uptake. *Annals of Botany*, *118*, 561–571.

Corso, D., Delzon, S., Lamarque, L. J., Cochard, H., Torres-Ruiz, J. M., King, A., & Brodribb, T. (2020). Neither xylem collapse, cavitation or changing leaf conductance drive stomatal closure in wheat. *Plant, Cell & Environment*, *43*, 854–865.

Couvreur, V., Vanderborght, J., & Javaux, M. (2012). A simple three-dimensional macroscopic root water uptake model based on the hydraulic architecture approach. *Hydrology and Earth System Sciences*, *16*, 2957–2971.

Deery, D. M., Passioura, J. B., Condon, J. R., & Katupitiya, A. (2013). Uptake of water from a Kandosol subsoil. II. Control of water uptake by roots. *Plant and Soil*, *368*, 649–667.

Dodd, I. C. (2005). Root-to-shoot Signalling: Assessing the roles of 'up' in the up and down world of long-distance Signalling in Planta. *Plant and Soil*, *274*, 251–270.

Gollan, T., Passioura, J. B., & Munns, R. (1986). Soil water status affects the stomatal conductance of fully turgid wheat and sunflower leaves. *Australian Journal of Plant Physiology*, *13*, 459–464.

Guo, K., Kong, W. W., & Yang, Z. M. (2009). Carbon monoxide promotes root hair development in tomato. *Plant, Cell & Environment*, *32*, 1033–1045.

Hayat, F., Ahmed, M. A., Zarebanadkouki, M., Cai, G., & Carminati, A. (2019). Measurements and simulation of leaf xylem water potential and root water uptake in heterogeneous soil water contents. *Advances in Water Resources*, *124*, 96–105.

Hayat, F., Ahmed, M. A., Zarebanadkouki, M., Javaux, M., Cai, G., & Carminati, A. (2020). Transpiration reduction in maize (*Zea mays* L) in response to soil drying. *Frontiers in Plant Science*, *10*. https://doi.org/10.3389/fpls.2019.01695.

Holbrook, N. M., Shashidhar, V. R., James, R. A., & Munns, R. (2002). Stomatal control in tomato with ABA-deficient roots: Response of grafted plants to soil drying. *Journal of Experimental Botany*, *53*, 1503–1514.

Martin-StPaul, N., Delzon, S., & Cochard, H. (2017). Plant resistance to drought depends on timely stomatal closure. *Ecology Letters*, *20*, 1437–1447.

Passioura, J. B. (1980). The transport of water from soil to shoot in wheat seedlings. *Journal of Experimental Botany*, *31*, 333–345.

Passioura, J. B., & Munns, R. (1984). Hydraulic resistance of plants. II. Effects of rooting medium, and time of day, in barley and Lupin. *Functional Plant Biology*, *11*, 341–350.

Peters, A., Iden, S. C., & Durner, W. (2015). Revisiting the simplified evaporation method: Identification of hydraulic functions considering vapor, film and corner flow. *Journal of Hydrology*, *527*, 531–542.

Rodriguez-Dominguez, C. M., & Brodribb, T. J. (2020). Declining root water transport drives stomatal closure in olive under moderate water stress. *New Phytologist*, *225*, 126–134.

Skelton, R. P., Brodribb, T. J., & Choat, B. (2017). Casting light on xylem vulnerability in an herbaceous species reveals a lack of segmentation. *New Phytologist*, *214*, 561–569.

Sperry, J. S., & Love, D. M. (2015). What plant hydraulics can tell us about responses to climate-change droughts. *New Phytologist*, *207*, 14–27.

Sperry, J. S., Wang, Y., Wolfe, B. T., Mackay, D. S., Anderegg, W. R. L., McDowell, N. G., & Pockman, W. T. (2016). Pragmatic hydraulic theory predicts stomatal responses to climatic water deficits. *New Phytologist*, *212*, 577–589.

van Genuchten, M. T. (1980). A closed-form equation for predicting the hydraulic conductivity of unsaturated soils. *Soil Science Society of America Journal*, *44*, 892–898.

SUPPORTING INFORMATION

Additional supporting information may be found online in the Supporting Information section at the end of this article.

How to cite this article: Abdalla M, Carminati A, Cai G, Javaux M, Ahmed MA. Stomatal closure of tomato under drought is driven by an increase in soil–root hydraulic resistance. *Plant Cell Environ.* 2021;44:425–431. https://doi.org/10.1111/pce.13939